Dynamic Systems Library Documentation

Audun Myers
Khasawneh Group, Mechanical Engineering, Michigan State University

December 8, 2020

Contents

1 Maps

1.1 Logistic Map

The logistic map [21] was generated as

$$x_{n+1} = rx_n(1 - x_n), \tag{1}$$

where we chose the parameters $x_0 = 0.5$ and $r = 3.6$ for a chaotic state. You can set $r = 3.5$ for a periodic response. We solve this system for 1000 data points and keep the second 500 to avoid transients. The resulting time series is shown below in Fig. 1.

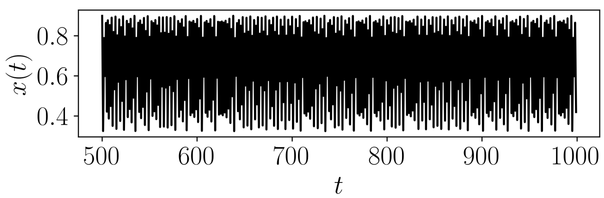

Figure 1

1.2 Hénon Map

The Hénon map [17] was solved as

$$\begin{aligned} x_{n+1} &= 1 - a x_n^2 + y_n, \\ y_{n+1} &= b x_n, \end{aligned} \tag{2}$$

where we chose the parameters $a = 1.20$, $b = 0.30$, and $c = 1.00$ for a chaotic state with initial conditions $x_0 = 0.1$ and $y_0 = 0.3$. You can set $a = 1.25$ for a periodic response. We solve this system for 1000 data points and keep the second 500 to avoid transients. The resulting time series is shown below in Fig. 2.

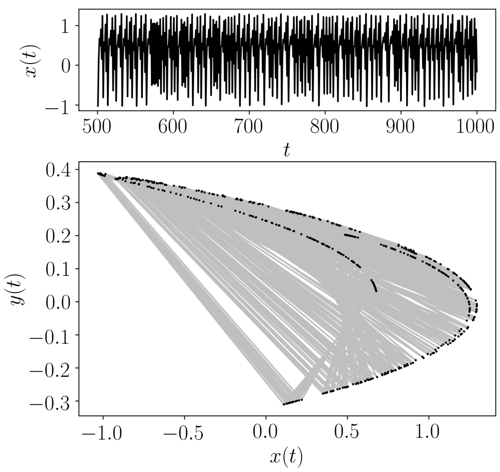

Figure 2

1.3 Sine Map

The Sine map is defined as

$$x_{n+1} = A\sin(\pi x_n) \tag{3}$$

where we chose the parameter $A = 1.0$ for a chaotic state with initial condition $x_0 = 0.1$. You can also change $A = 0.8$ for a periodic response. We solve this system for 1000 data points and keep the second 500 to avoid transients. The resulting time series is shown below in Fig. 3.

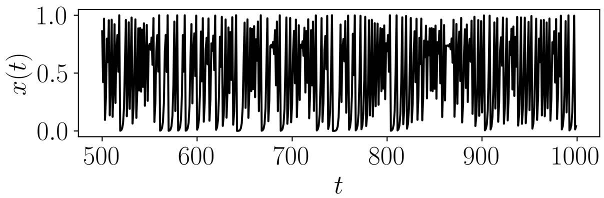

Figure 3

1.4 Tent Map

The Tent map is defined [10] as

$$x_{n+1} = A \min([x_n, 1 - x_n]) \tag{4}$$

where we chose the parameter $A = 1.50$ for a chaotic state with initial condition $x_0 = 1/\sqrt{2}$. You can also change $A = 1.05$ for a periodic response. We solve this system for 1000 data points and keep the second 500 to avoid transients. The resulting time series is shown below in Fig. 4.

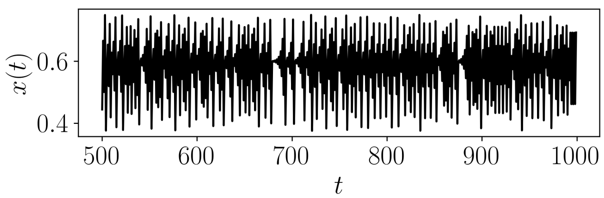

Figure 4

1.5 Linear Congruential Generator Map

The Linear Congruential Generator map is defined as

$$x_{n+1} = A \min([x_n, 1 - x_n]) \tag{5}$$

where we chose the parameters $a = 1.1$, $b = 54773$, and $c = 259200$ for a chaotic state with initial condition $x_0 = 0.1$. You can set $a = 1.1$ for a periodic response. We solve this system for 1000 data points and keep the second 500 to avoid transients. The resulting time series is shown below in Fig. 5.

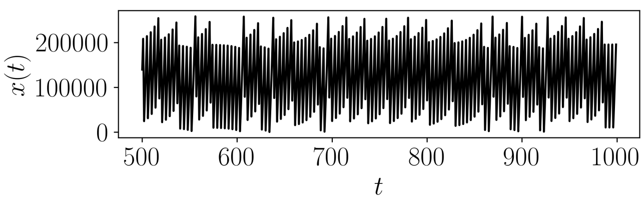

Figure 5

1.6 Ricker's Population Map

The Ricker's Population map is defined [23] as

$$x_{n+1} = ax_n e^{-x_n} \tag{6}$$

where we chose the parameter $a = 20$ for a chaotic state with initial condition $x_0 = 0.1$. You can set $a = 13$ for a periodic response. We solve this system for 1000 data points and keep the second 500 to avoid transients. The resulting time series is shown below in Fig. 6.

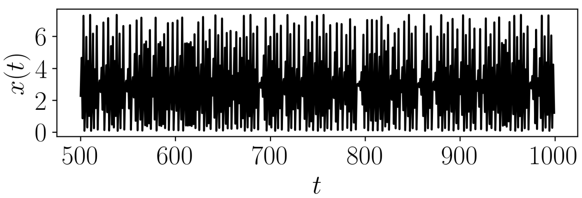

Figure 6

1.7 Gauss Map

The Gauss map is defined [18] as

$$x_{n+1} = e^{-\alpha x_n^2} + \beta \tag{7}$$

where we chose the parameters $\alpha = 6.20$ and $\beta = -0.35$ for a chaotic state with initial condition $x_0 = 0.1$. You can set $\beta = -0.20$ for a periodic response. We solve this system for 1000 data points and keep the second 500 to avoid transients. The resulting time series is shown below in Fig. 7.

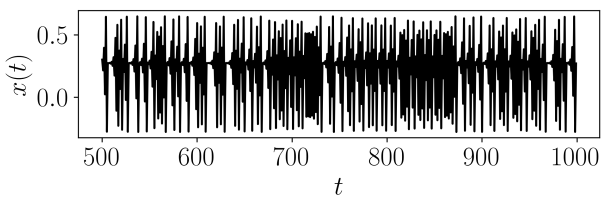

Figure 7

1.8 Cusp Map

The Cusp map is defined [5] as

$$x_{n+1} = 1 - a\sqrt{|x_n|} \tag{8}$$

where we chose the parameter $a = 1.2$ for a chaotic state with initial condition $x_0 = 0.5$. You can set $a = 1.1$ for a periodic response. We solve this system for 1000 data points and keep the second 500 to avoid transients. The resulting time series is shown below in Fig. 8.

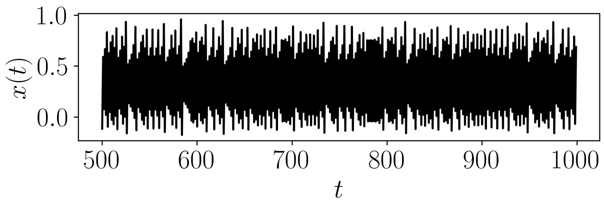

Figure 8

1.9 Pincher's Map

The Pincher's map is defined [?] as

$$x_{n+1} = |\tanh(s(x_n - c)| \tag{9}$$

where we chose the parameters $s = 1.6$ and $c = 0.5$ for a chaotic state with initial condition $x_0 = 0.0$. You can set $s = 1.3$ for a periodic response. We solve this system for 1000 data points and keep the second 500 to avoid transients. The resulting time series is shown below in Fig. 10.

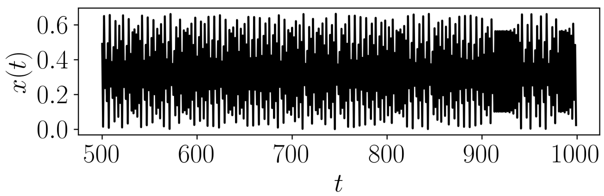

Figure 9

1.10 Sine Circle Map

The Sine Circle map is defined [3] as

$$x_{n+1} = x_n + \omega - \left[\frac{k}{2\pi}\sin(2\pi x_n)\right](\text{mod}1) \tag{10}$$

where we chose the parameters $\omega = 0.5$ and $k = 2.0$ for a chaotic state with initial condition $x_0 = 0.0$. You can set $k = 1.5$ for a periodic response. We solve this system for 1000 data points and keep the second 500 to avoid transients. The resulting time series is shown below in Fig. 10.

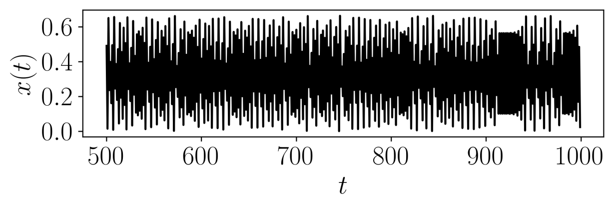

Figure 10

1.11 Lozi Map

The Lozi map is defined [14] as

$$
\begin{aligned}
x_{n+1} &= 1 - a|x_n| + by_n \\
y_{n+1} &= x_n
\end{aligned}
\tag{11}
$$

where we chose the parameters $a = 1.7$ and $b = 0.5$ for a chaotic state with initial conditions $x_0 = -0.1$ and $y_0 = 0.1$. You can set $a = 1.5$ for a periodic response. We solve this system for 1000 data points and keep the second 500 to avoid transients. The resulting time series is shown below in Fig. 11.

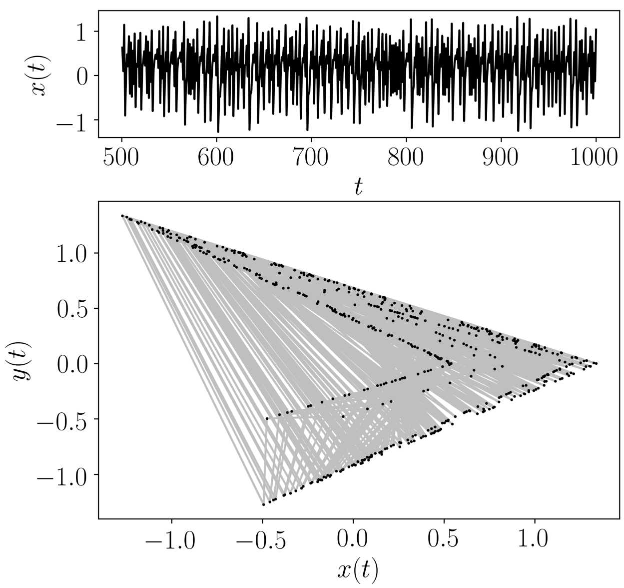

Figure 11

1.12 Delayed Logistic Map

The Delayed Logistic map is defined [**?**] as

$$\begin{aligned} x_{n+1} &= a x_n (1 - y_n) \\ y_{n+1} &= x_n \end{aligned} \tag{12}$$

where we chose the parameter $a = 2.27$ for a chaotic state with initial conditions $x_0 = 0.001$ and $y_0 = 0.001$. You can set $a = 2.20$ for a periodic response. We solve this system for 1000 data points and keep the second 500 to avoid transients. The resulting time series is shown below in Fig. 12.

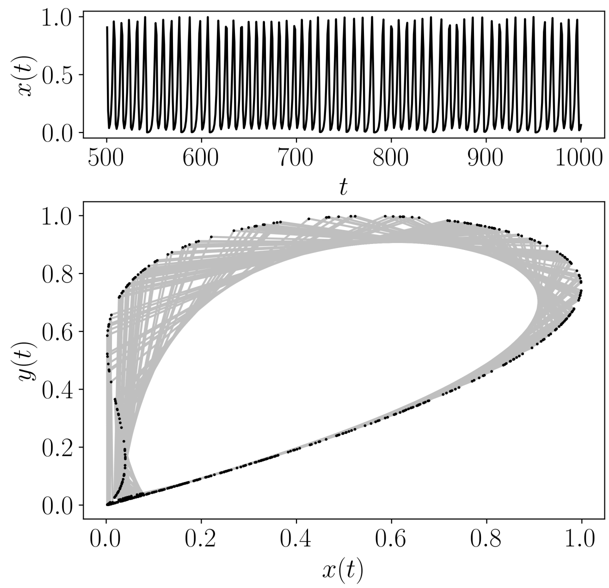

Figure 12

1.13 Tinkerbell Map

The Tinkerbell map is defined [16] as

$$
\begin{aligned}
x_{n+1} &= x_n^2 - y_n^2 + a x_n + b y_n \\
y_{n+1} &= 2 x_n y_n + c x_n + d y_n
\end{aligned}
\tag{13}
$$

where we chose the parameters $a = 0.9$, $b = -0.6$, $c = 2.0$, and $d = 0.5$ for a chaotic state with initial conditions $x_0 = 0.0$ and $y_0 = 0.5$. You can set $a = 0.7$ for a periodic response. We solve this system for 1000 data points and keep the second 500 to avoid transients. The resulting time series is shown below in Fig. 13.

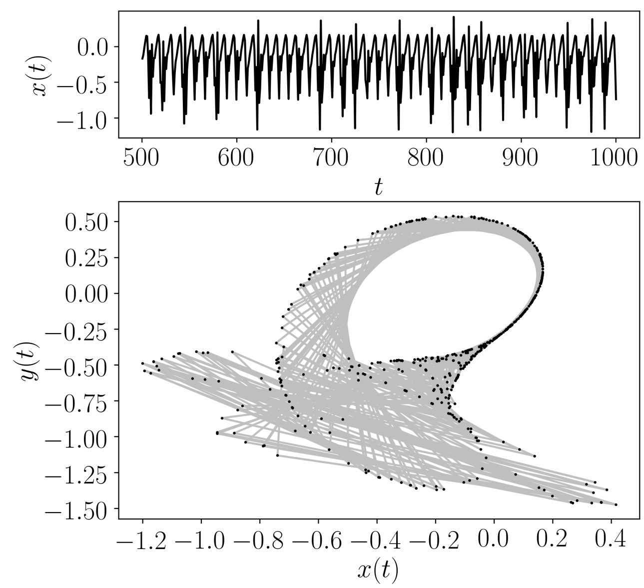

Figure 13

1.14 Burger's Map

The Burger's map is defined [6] as

$$
\begin{aligned}
x_{n+1} &= a x_n - y_n^2 \\
y_{n+1} &= b y_n + x_n y_n
\end{aligned}
\tag{14}
$$

where we chose the parameters $a = 0.75$ and $b = 1.75$ for a chaotic state with initial conditions $x_0 = -0.1$ and $y_0 = 0.5$. You can set $b = 1.60$ for a periodic response. We solve this system for 1000 data points and keep the second 500 to avoid transients. The resulting time series is shown below in Fig. 14.

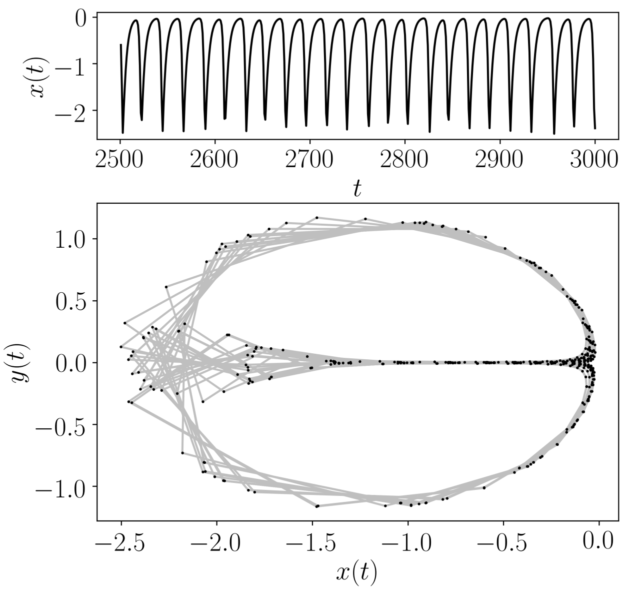

Figure 14

1.15 Holme's Cubic Map

The Holme's Cubic map is defined [8] as

$$
\begin{aligned}
x_{n+1} &= y_n \\
y_{n+1} &= -bx_n + dy_n - y_n^3
\end{aligned}
\tag{15}
$$

where we chose the parameters $b = 0.20$ and $d = 2.77$ for a chaotic state with initial conditions $x_0 = -0.1$ and $y_0 = 0.5$. You can set $b = 0.27$ for a periodic response. We solve this system for 1000 data points and keep the second 500 to avoid transients. The resulting time series is shown below in Fig. 15.

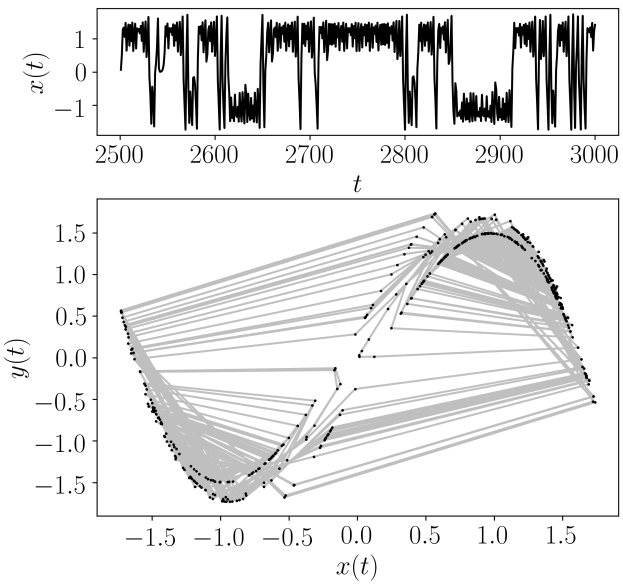

Figure 15

1.16 Kaplan Yorke Map

The Kaplan Yorke map is defined [19] as

$$\begin{aligned} x_{n+1} &= [ax_n]\,(\text{mod} 1) \\ y_{n+1} &= by_n + \cos(4\pi x_n) \end{aligned} \tag{16}$$

where we chose the parameters $a = -2.0$ and $b = 0.2$ for a chaotic state with initial conditions $x_0 = -0.1$ and $y_0 = 0.5$. You can set $a = -1.0$ for a periodic response. We solve this system for 1000 data points and keep the second 500 to avoid transients. The resulting time series is shown below in Fig. 16.

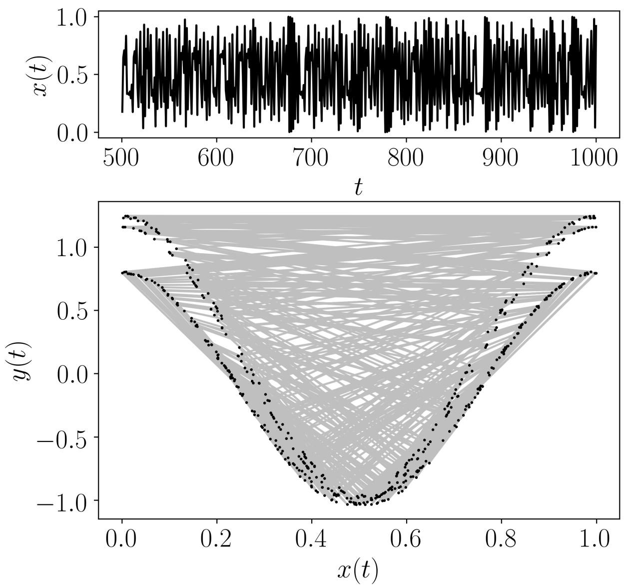

Figure 16

1.17 Gingerbread Man Map

The Gingerbread Man Map is defined [12, 13] as

$$\begin{aligned} x_{n+1} &= 1 - a y_n + n|x_n| \\ y_{n+1} &= x_n \end{aligned} \tag{17}$$

where we chose the parameters $a = 1.0$ and $b = 1.0$. For a chaotic state, initial conditions $x_0 = 0.5$ and $y_0 = 1.8$, and for a periodic response $x_0 = 0.5$ and $y_0 = 1.5$. We solve this system for 2000 data points and keep the last 500 to avoid transients. The resulting time series is shown below in Fig. 17.

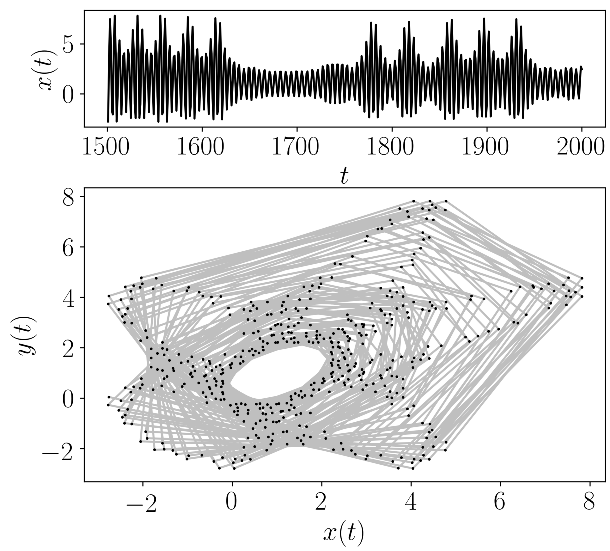

Figure 17

2 Autonomous Dissipative Flows

The continuous differential equations were simulated using the *odeint* function from the *Scipy* library of Python with default function parameters.

2.1 Lorenz System

The Lorenz system used is defined as

$$\frac{dx}{dt} = \sigma(y - x),\ \frac{dy}{dt} = x(\rho - z) - y,\ \frac{dz}{dt} = xy - \beta z. \tag{18}$$

The Lorenz system was solved with a sampling rate of 100 Hz for 100 seconds with only the last 20 seconds used to avoid transients. For a chaotic response, parameters of $\sigma = 10.0$, $\beta = 8.0/3.0$, and $\rho = 105$ and initial conditions $[x_0, y_0, z_0] = [10^{-10}, 0, 1]$ are used (see Fig. 18). For a periodic response set $\rho = 100$.

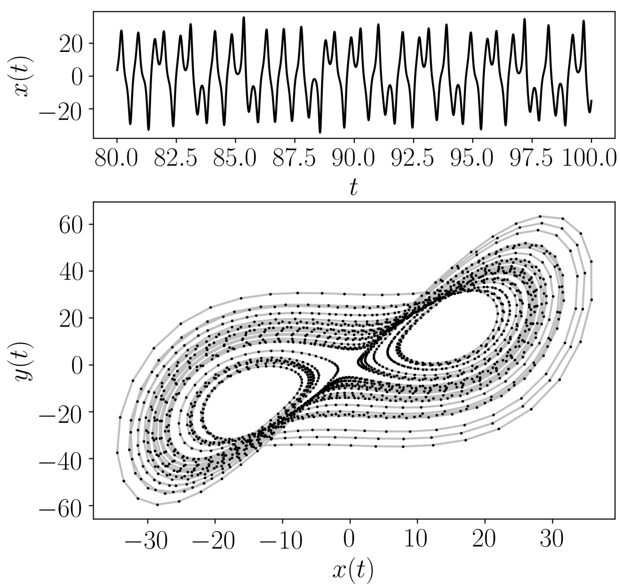

Figure 18

2.2 Rössler System

The Rössler system used was defined as

$$\frac{dx}{dt} = -y - z, \ \frac{dy}{dt} = x + ay, \ \frac{dz}{dt} = b + z(x - c), \tag{19}$$

The Lorenz system was solved with a sampling rate of 15 Hz for 1000 seconds with only the last 170 seconds used to avoid transients. For a chaotic response, parameters of $a = 0.15$, $b = 0.2$, and $c = 14$ and initial conditions $[x_0, y_0, z_0] = [-0.4, 0.6, 1.0]$ are used (see Fig. 19). For a periodic response set $a = 0.10$.

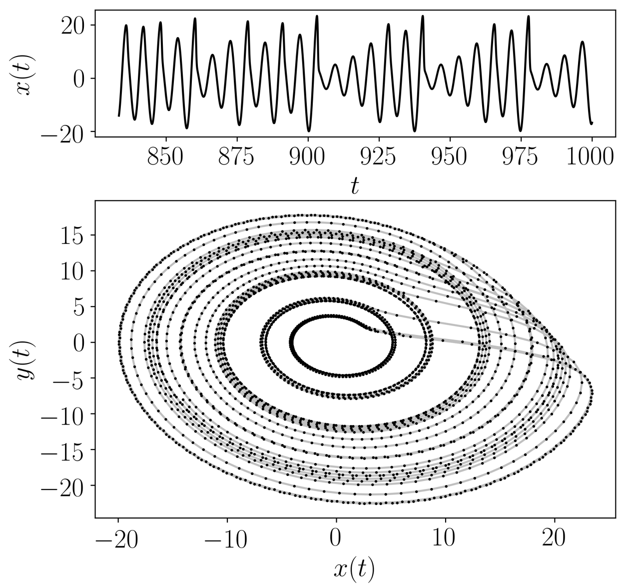

Figure 19

2.3 Coupled Rössler-Lorenz System

The coupled Lorenz-Rössler system is defined as

$$
\begin{aligned}
\frac{dx_1}{dt} &= -y_1 - z_1 + k_1(x_2 - x_1), \\
\frac{dy_1}{dt} &= x_1 + ay_1 + k_2(y_2 - y_1), \\
\frac{dz_1}{dt} &= b_2 + z_1(x_1 - c_2) + k_3(z_2 - z_1), \\
\frac{dx_2}{dt} &= \sigma(y_2 - x_2), \\
\frac{dy_2}{dt} &= \lambda x_2 - y_2 - x_2 z_2, \\
\frac{dz_2}{dt} &= x_2 y_2 - b_1 z_2,
\end{aligned}
\tag{20}
$$

where $b_1 = 8/3$, $b_2 = 0.2$, $c_2 = 5.7$, $k_1 = 0.1$, $k_2 = 0.1$, $k_3 = 0.1$, $\lambda = 28$, $\sigma = 10$, and $a = 0.25$ for a periodic response and $a = 0.51$ for a chaotic response. This system was simulated at a frequency of 50 Hz for 500 seconds with the last 300 seconds used as shown in Fig. 24.

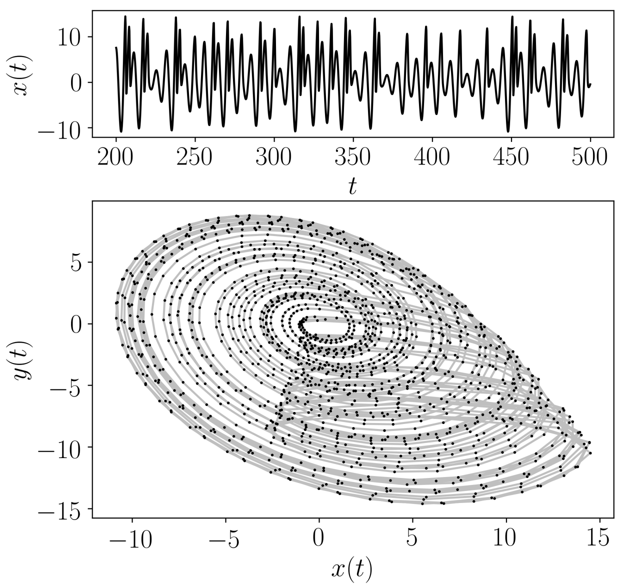

Figure 20

2.4 Bi-Directional Coupled Rössler System

The Bi-directional Rössler system is defined as

$$\begin{aligned}
\frac{dx_1}{dt} &= -w_1 y_1 - z_1 + k(x_2 - x_1),\\
\frac{dy_1}{dt} &= w_1 x_1 + 0.165 y_1,\\
\frac{dz_1}{dt} &= 0.2 + z_1(x_1 - 10),\\
\frac{dx_2}{dt} &= -w_2 y_2 - z2 + k(x_1 - x_2),\\
\frac{dy_2}{dt} &= w_2 x_2 + 0.165 y_2,\\
\frac{dz_2}{dt} &= 0.2 + z_2(x_2 - 10),
\end{aligned} \tag{21}$$

with $w_1 = 0.99$, $w_2 = 0.95$, and $k = 0.05$. This was solved for 1000 seconds with a sampling rate of 10 Hz. Only the last 140 seconds of the solution are used as shown in Fig. 25.

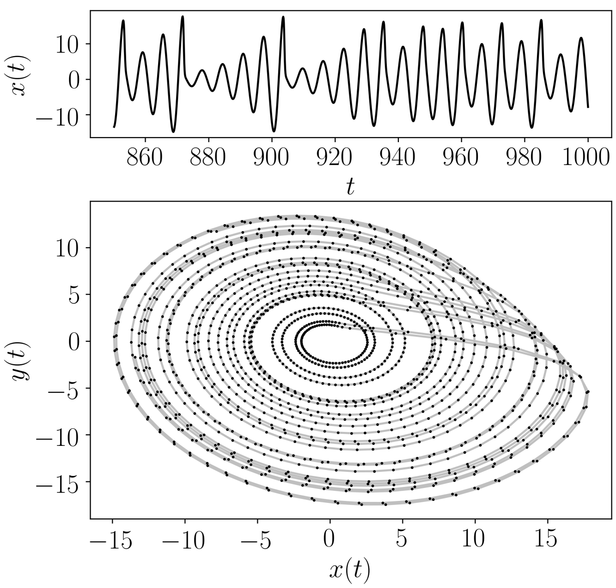

Figure 21

2.5 Chua Circuit

Chua's circuit is based on a non-linear circuit and is described as

$$\begin{aligned}
\frac{dx}{dt} &= \alpha(y - f(x)), \\
\frac{dy}{dt} &= \gamma(x - y + z), \\
\frac{dz}{dt} &= -\beta y,
\end{aligned} \tag{22}$$

where $f(x)$ is based on a non-linear resistor model defined as

$$f(x) = m_1 x + \frac{1}{2}(m_0 + m_1)\left[|x+1| - |x-1|\right]. \tag{23}$$

The system parameters are set to $\beta = 27$, $\gamma = 1$, $m_0 = -3/7$, $m_1 = 3/7$, and $\alpha = 10.8$ for a periodic response and $\alpha = 12.8$ for a chaotic response. The system was simulated for 200 seconds at a rate of 50 Hz and the last 80 seconds were used for the chaotic response shown in Fig. 22.

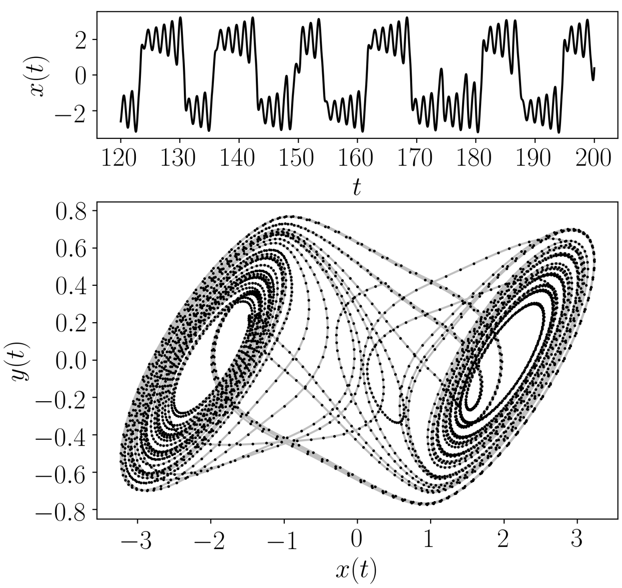

Figure 22

2.6 Double Pendulum

The double pendulum is a staple benchtop experiment for investigated chaos in a mechanical system. A point-mass double pendulum's equations of motion are defined as shown in Eq. (24), where the system

$$\begin{aligned}
\frac{d\theta_1}{dt} &= \omega_1, \\
\frac{d\theta_2}{dt} &= \omega_2, \\
\frac{d\omega_1}{dt} &= \frac{-g(2m_1+m_2)\mathrm{s}(\theta_1) - m_2\mathrm{s}(\theta_1-2\theta_2) - 2\mathrm{s}(\theta_1-\theta_2)m_2\left(\omega_2^2\ell_2 + \omega_1^2\ell_1\mathrm{c}(\theta_1-\theta_2)\right)}{\ell_1(2m_1+m_2-m_2\mathrm{c}(2\theta_1-2\theta_2)}, \\
\frac{d\omega_2}{dt} &= \frac{2\mathrm{s}(\theta_1-\theta_2)\left(\omega_1^2\ell_1(m_1+m_2) + g(m_2+m_2)\mathrm{c}(\theta_1) + \omega_2^2\ell_2 m_2\mathrm{c}(\theta_1-\theta_2)\right)}{\ell_2(2m_1+m_2-m_2\mathrm{c}(2\theta_1-2\theta_2)}.
\end{aligned} \tag{24}$$

parameters are $g = 9.81$ m/s^2, $m_1 = 1$ kg, $m_2 = 1$ kg, $\ell_1 = 1$ m, and $\ell_2 = 1$ m. The system was solved for 200 seconds at a rate of 100 Hz and only the last 30 seconds were used as shown in the figure below for the chaotic response with initial conditions $[\theta_1, \theta_2, \omega_1, \omega_2] = [0, 3\,\mathrm{rad}, 0, 0]$. This system will have different dynamic states based on the initial conditions, which can vary from periodic, quasiperiodic, and chaotic.

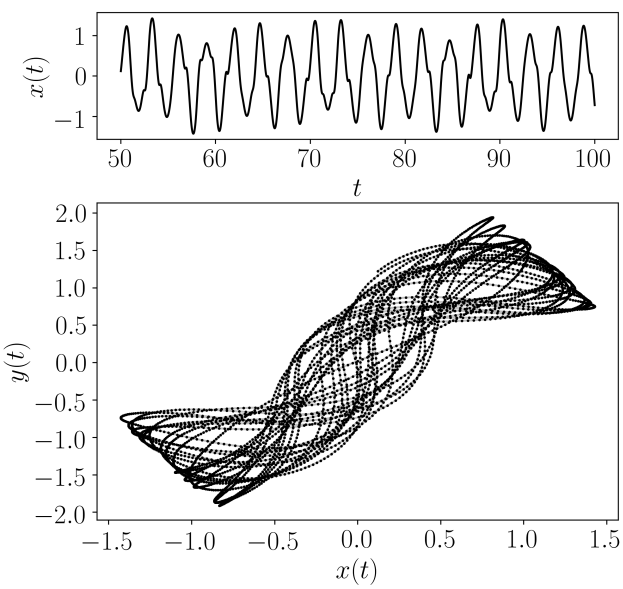

Figure 23

2.7 Diffusionless Lorenz

The Diffusionless Lorenz attractor is defined as

$$\begin{aligned} \frac{dx}{dt} &= -y - x, \\ \frac{dy}{dt} &= -xz, \\ \frac{dz}{dt} &= xy + R, \end{aligned} \tag{25}$$

The system parameter is set to $R = 0.40$ for a chaotic response and $R = 0.25$ for a periodic response. The initial conditions were set to $[x, y, z] = [1.0, -1.0, 0.01]$. The system was simulated for 1000 seconds at a rate of 40 Hz and the last 250 seconds were used for the chaotic response shown in Fig. 26.

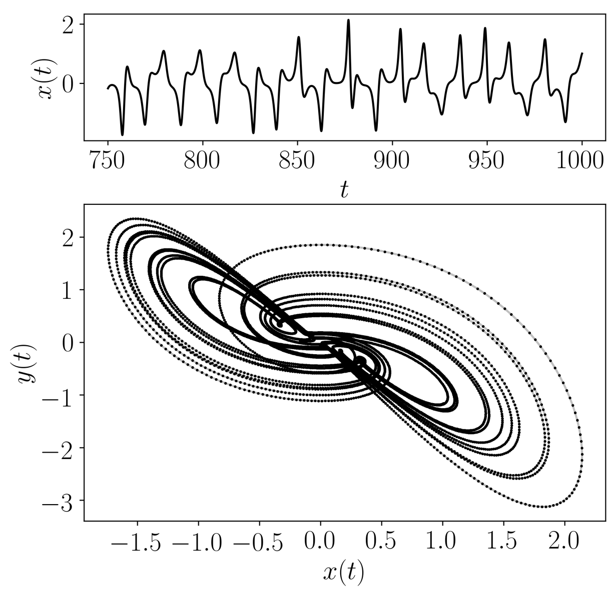

Figure 24

2.8 Complex Butterfly

The Complex Butterfly attractor is defined as

$$\begin{aligned} \frac{dx}{dt} &= a(y-x), \\ \frac{dy}{dt} &= z\mathrm{sgn}(x), \\ \frac{dz}{dt} &= |x|-1, \end{aligned} \tag{26}$$

The system parameter is set to $a = 0.55$ for a chaotic response and $a = 0.15$ for a periodic response. The initial conditions were set to $[x, y, z] = [0.2, 0.0, 0.0]$. The system was simulated for 1000 seconds at a rate of 10 Hz and the last 500 seconds were used for the chaotic response shown in Fig. 27.

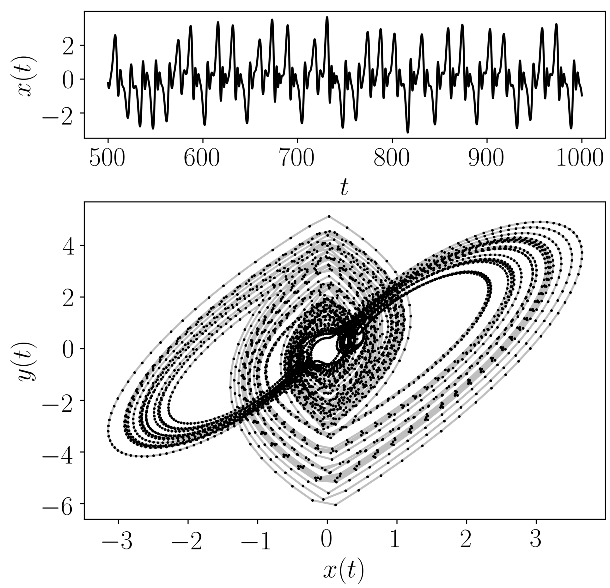

Figure 25

2.9 Chen's System

Chen's System is defined [?] as

$$\frac{dx}{dt} = a(y - x),$$
$$\frac{dy}{dt} = (c - a)x - xz + cy, \quad (27)$$
$$\frac{dz}{dt} = xy - bz,$$

The system parameters are set to $a = 35$, $b = 3$, and $c = 28$ for a chaotic response and $a = 30$ for a periodic response. The initial conditions were set to $[x, y, z] = [-10, 0, 37]$. The system was simulated for 500 seconds at a rate of 200 Hz and the last 15 seconds were used for the chaotic response shown in Fig. 28.

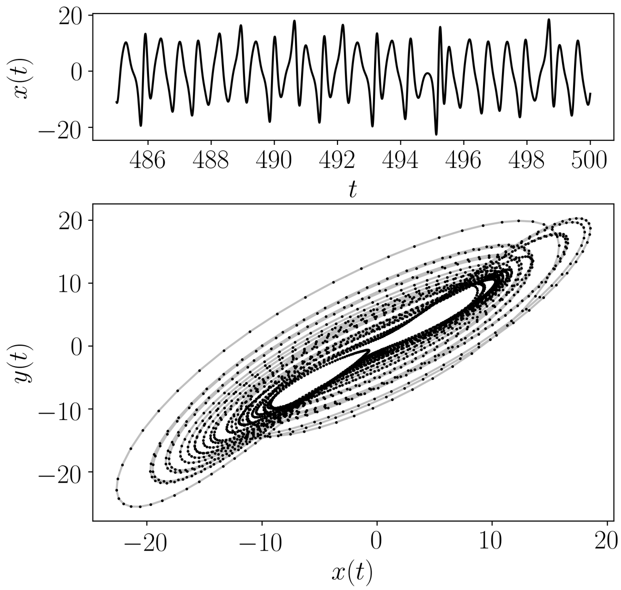

Figure 26

2.10 Hadley Circulation

The Hadley Circulation system is defined as

$$\begin{aligned}\frac{dx}{dt} &= -y^2 - z^2 - ax + aF,\\ \frac{dy}{dt} &= xy - bxz - y + G,\\ \frac{dz}{dt} &= bxy + xz - z,\end{aligned} \tag{28}$$

Dynamics	**Initial Cond.**	**Parameters**	**Sample Freq. (Hz)**	**Sample Domain**
Chaotic	$[x_0, y_0] = [-10, 0, 37]$	$[a, b, F, G] = [0.3, 4, 8, 1]$	50	[21000, 25000]
Periodic	$[x_0, y_0] = [-10, 0, 37]$	$[a, b, F, G] = [0.25, 4, 8, 1]$		

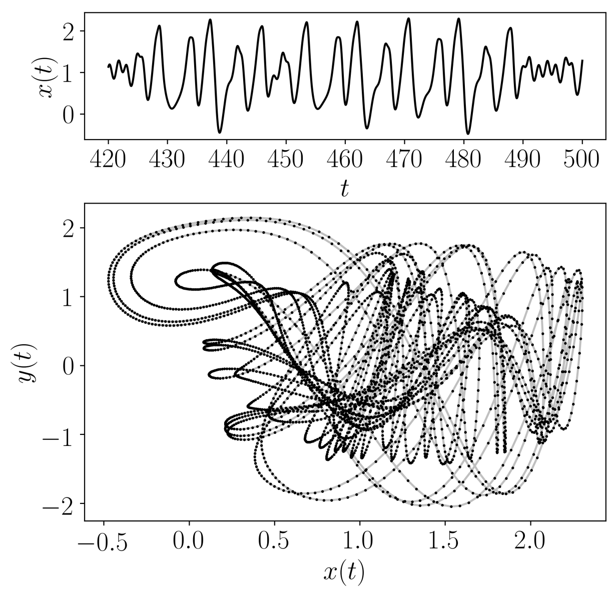

Figure 27

2.11 ACT Attractor

The ACT attractor is defined [2] as

$$\begin{aligned}
\frac{dx}{dt} &= \alpha(x - y), \\
\frac{dy}{dt} &= -4\alpha y + xz + \mu x^3, \\
\frac{dz}{dt} &= -\delta\alpha z + xy + \beta z^2,
\end{aligned} \tag{29}$$

Dynamics	**Initial Cond.**	**Parameters**	**Sample Freq. (Hz)**	**Sample Domain**
Chaotic	$[x_0, y_0, z_0] = [0.5, 0, 0]$	$[\alpha, \mu, \delta, \beta] = [2.0, 0.02, 1.5, -0.07]$	50	[21000, 25000]
Periodic	$[x_0, y_0, z_0] = [0.5, 0, 0]$	$[\alpha, \mu, \delta, \beta] = [2.5, 0.02, 1.5, -0.07]$		

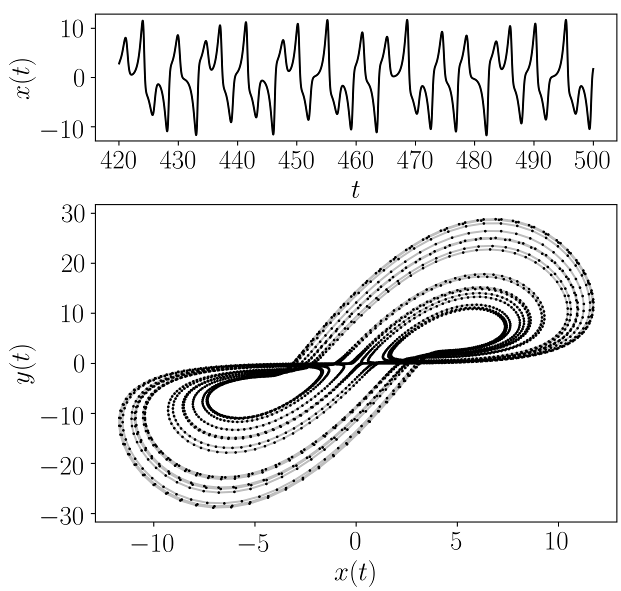

Figure 28

2.12 Rabinovich-Frabrikant Attractor

The Rabinovich-Frabrikant attractor is defined [11] as

$$\begin{aligned}\frac{dx}{dt} &= \alpha(x-y),\\ \frac{dy}{dt} &= -4\alpha y + xz + \mu x^3,\\ \frac{dz}{dt} &= -\delta\alpha z + xy + \beta z^2,\end{aligned} \tag{30}$$

Dynamics	**Initial Cond.**	**Parameters**	**Sample Freq. (Hz)**	**Sample Domain**
Chaotic	$[x_0, y_0, z_0] = [-1, 0, 0.5]$	$[\alpha, \gamma] = [1.13, 0.87]$	30	[12000, 15000]
Periodic	$[x_0, y_0, z_0] = [-1, 0, 0.5]$	$[\alpha, \gamma] = [1.16, 0.87]$		

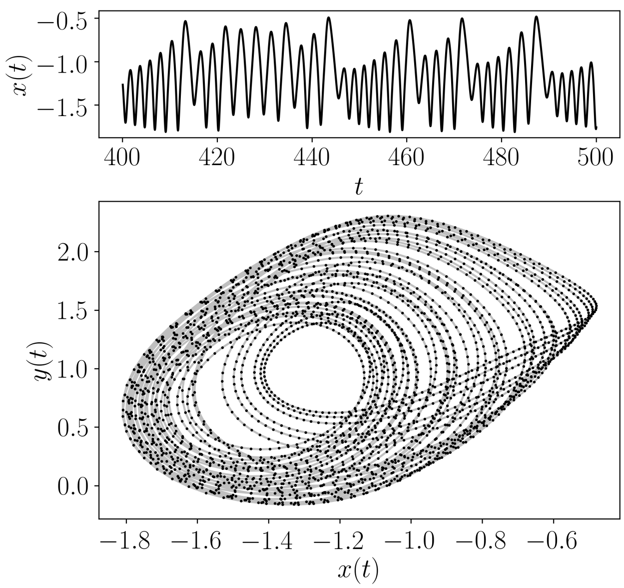

Figure 29

2.13 Linear-Feedback of Rigid-Body-Motion System

The Linear-Feedback of Rigid-Body-Motion System is defined [9] as

$$\begin{aligned} \frac{dx}{dt} &= -yz + ax, \\ \frac{dy}{dt} &= xz + by, \\ \frac{dz}{dt} &= \frac{1}{3}xy + cz, \end{aligned} \tag{31}$$

Dynamics	**Initial Cond.**	**Parameters**	**Sample Freq. (Hz)**	**Sample Domain**
Chaotic	$[x_0, y_0, z_0] = [0.2, 0.2, 0.2]$	$[a, b, c] = [5.0, -10, -3.8]$	100	[47000, 50000]
Periodic	$[x_0, y_0, z_0] = [0.2, 0.2, 0.2]$	$[a, b, c] = [5.3, -10, -3.8]$		

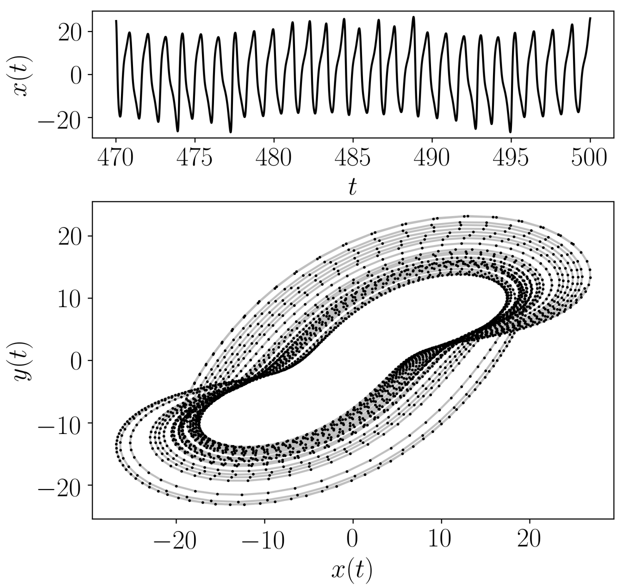

Figure 30

2.14 Moore-Spiegel Oscillator

The Moore-Spiegel Oscillator is defined [4] as

$$\begin{aligned}\frac{dx}{dt} &= y,\\ \frac{dy}{dt} &= z,\\ \frac{dz}{dt} &= -z-(T-R+Rx^2)y-Tx,\end{aligned} \tag{32}$$

Dynamics	Initial Cond.	Parameters	Sample Freq. (Hz)	Sample Domain
Chaotic	$[x_0, y_0, z_0] = [0.2, 0.2, 0.2]$	$[T, R] = [7.0, 20]$	100	[45000, 50000]
Periodic	$[x_0, y_0, z_0] = [0.2, 0.2, 0.2]$	$[T, R] = [7.8, 20]$		

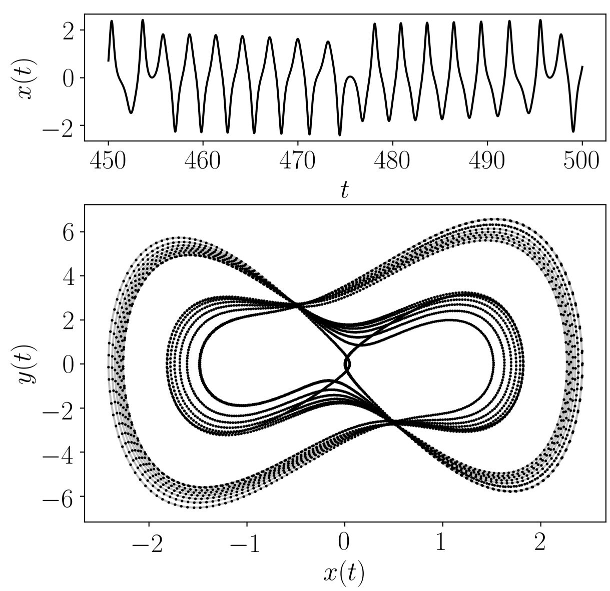

Figure 31

2.15 Thomas Cyclically Symmetric Attractor

The Thomas Cyclically Symmetric Attractor is defined [26] as

$$\begin{aligned}\frac{dx}{dt} &= -bx + \sin(y),\\ \frac{dy}{dt} &= -by + \sin(z),\\ \frac{dz}{dt} &= -bz + \sin(x),\end{aligned} \tag{33}$$

Dynamics	**Initial Cond.**	**Parameters**	**Sample Freq. (Hz)**	**Sample Domain**
Chaotic	$[x_0, y_0, z_0] = [0.1, 0, 0]$	$[b] = [0.18]$	10	[5000, 10000]
Periodic	$[x_0, y_0, z_0] = [0.1, 0, 0]$	$[b] = [0.17]$		

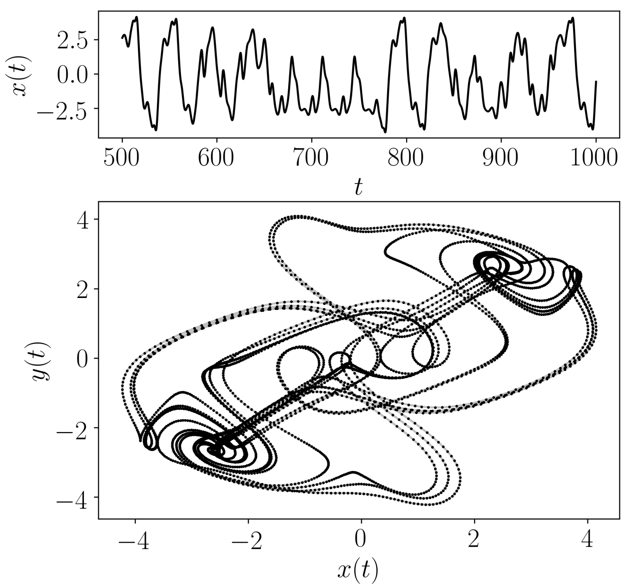

Figure 32

2.16 Halvorsens Cyclically Symmetric Attractor

The Halvorsens Cyclically Symmetric Attractor is defined as

$$\begin{aligned}\frac{dx}{dt} &= -ax - by - cz - y^2,\\ \frac{dy}{dt} &= -ay - bz - cx - z^2,\\ \frac{dz}{dt} &= -az - bx - cy - x^2,\end{aligned} \tag{34}$$

Dynamics	Initial Cond.	Parameters	Sample Freq. (Hz)	Sample Domain
Chaotic	$[x_0, y_0, z_0] = [-5, 0, 0]$	$[a, b, c] = [1.45, 4, 4]$	200	[35000, 40000]
Periodic	$[x_0, y_0, z_0] = [-5, 0, 0]$	$[a, b, c] = [1.85, 4, 4]$		

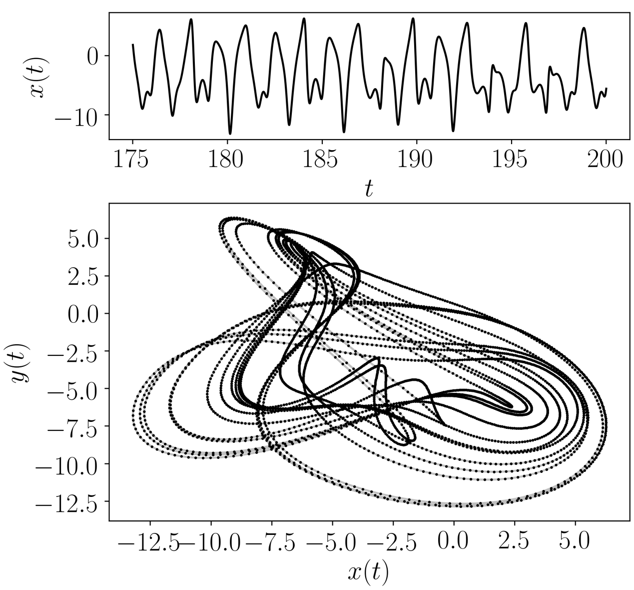

Figure 33

2.17 Burke-Shaw Attractor

The Burke-Shaw Attractor is defined [24] as

$$\begin{aligned}\frac{dx}{dt} &= -s(x+y),\\ \frac{dy}{dt} &= -y - sxz,\\ \frac{dz}{dt} &= sxy + V,\end{aligned} \tag{35}$$

Dynamics	Initial Cond.	Parameters	Sample Freq. (Hz)	Sample Domain
Chaotic	$[x_0, y_0, z_0] = [0.6, 0, 0]$	$[s] = [10]$	200	[95000, 100000]
Periodic	$[x_0, y_0, z_0] = [0.6, 0, 0]$	$[s] = [12]$		

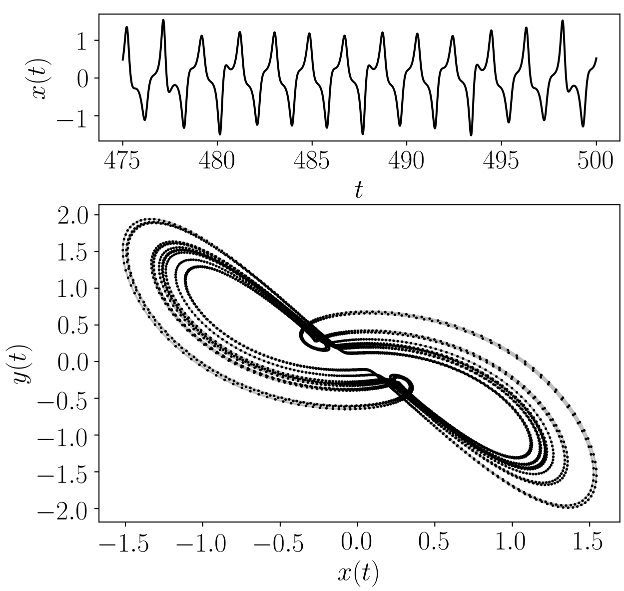

Figure 34

2.18 Rucklidge Attractor

The Rucklidge Attractor is defined [7] as

$$\begin{aligned}\frac{dx}{dt} &= -kx + \lambda y - yz,\\ \frac{dy}{dt} &= x,\\ \frac{dz}{dt} &= -z + y^2,\end{aligned} \tag{36}$$

Dynamics	Initial Cond.	Parameters	Sample Freq. (Hz)	Sample Domain
Chaotic	$[x_0, y_0, z_0] = [1, 0, 4.5]$	$[k, \lambda] = [1.6, 6.7]$	50	[45000, 50000]
Periodic	$[x_0, y_0, z_0] = [1, 0, 4.5]$	$[k, \lambda] = [1.1, 6.7]$		

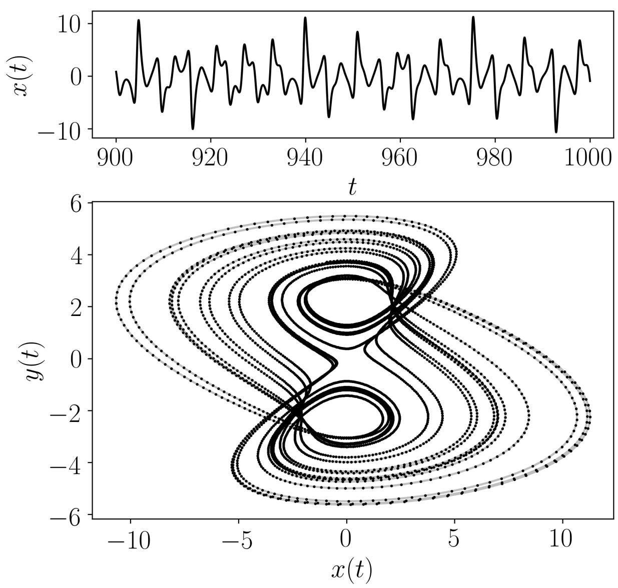

Figure 35

2.19 WINDMI Attractor

The WINDMI Attractor is defined [27] as

$$\begin{aligned}\frac{dx}{dt} &= y,\\ \frac{dy}{dt} &= z,\\ \frac{dz}{dt} &= -az - y + b - e^x,\end{aligned} \tag{37}$$

Dynamics	**Initial Cond.**	**Parameters**	**Sample Freq. (Hz)**	**Sample Domain**
Chaotic	$[x_0, y_0, z_0] = [1, 0, 4.5]$	$[a, b] = [0.8, 2.5]$	20	[15000, 20000]
Periodic	$[x_0, y_0, z_0] = [1, 0, 4.5]$	$[a, b] = [0.9, 2.5]$		

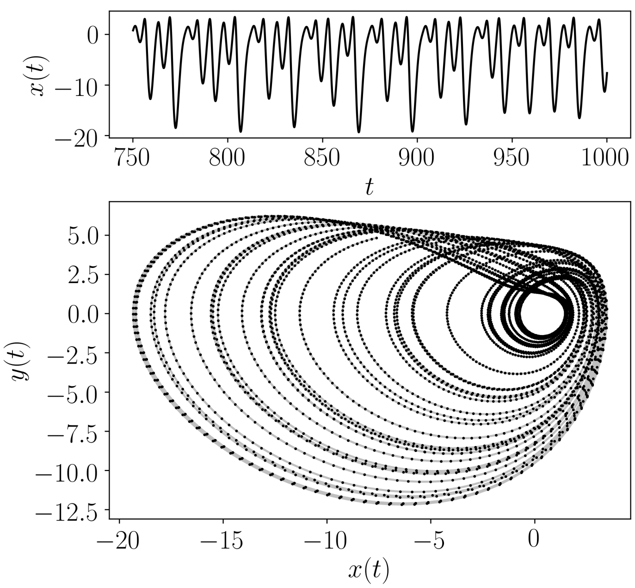

Figure 36

2.20 Simplest Quadratic Chaotic Flow

The Simplest Quadratic Chaotic Flow is defined [25] as

$$\begin{aligned}\frac{dx}{dt} &= y,\\ \frac{dy}{dt} &= z,\\ \frac{dz}{dt} &= -az - y + b - e^{x},\end{aligned} \tag{38}$$

Dynamics	Initial Cond.	Parameters	Sample Freq. (Hz)	Sample Domain
Chaotic	$[x_0, y_0, z_0] = [-0.9, 0, 0.5]$	$[a, b] = [2.017, 1]$	20	[15000, 20000]
Periodic	$[x_0, y_0, z_0] = [-0.9, 0, 0.5]$	$[a, b] = [\text{NA}]$		

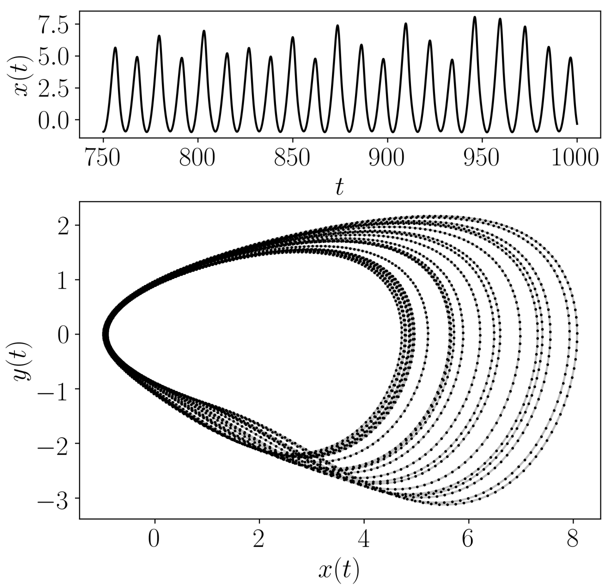

Figure 37

2.21 Simplest Cubic Chaotic Flow

The Simplest Cubic Chaotic Flow is defined [20] as

$$\begin{aligned} \frac{dx}{dt} &= y, \\ \frac{dy}{dt} &= z, \\ \frac{dz}{dt} &= -az + xy^2 - x, \end{aligned} \tag{39}$$

Dynamics	Initial Cond.	Parameters	Sample Freq. (Hz)	Sample Domain
Chaotic	$[x_0, y_0, z_0] = [0, 0.96, 0]$	$[a, b] = [2.05, 2.5]$	20	[15000, 20000]
Periodic	$[x_0, y_0, z_0] = [0, 0.96, 0]$	$[a, b] = [2.11, 2.5]$		

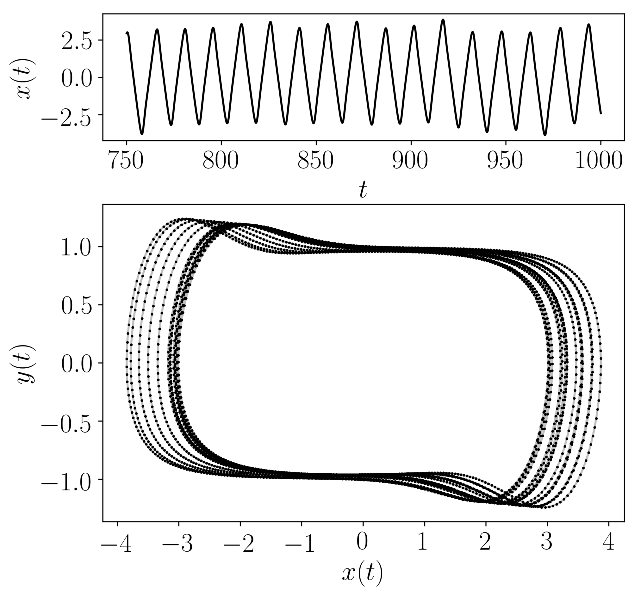

Figure 38

2.22 Simplest Piecewise-Linear Chaotic Flow

The Simplest Piecewise-Linear Chaotic Flow is defined [28] as

$$\begin{aligned}\frac{dx}{dt} &= y,\\ \frac{dy}{dt} &= z,\\ \frac{dz}{dt} &= -az - y + |x| - 1,\end{aligned} \tag{40}$$

Dynamics	**Initial Cond.**	**Parameters**	**Sample Freq. (Hz)**	**Sample Domain**
Chaotic	$[x_0, y_0, z_0] = [0, -0.7, 0]$	$[a] = [0.6]$	40	[35000, 40000]
Periodic	$[x_0, y_0, z_0] = [0, -0.7, 0]$	$[a] = [0.7]$		

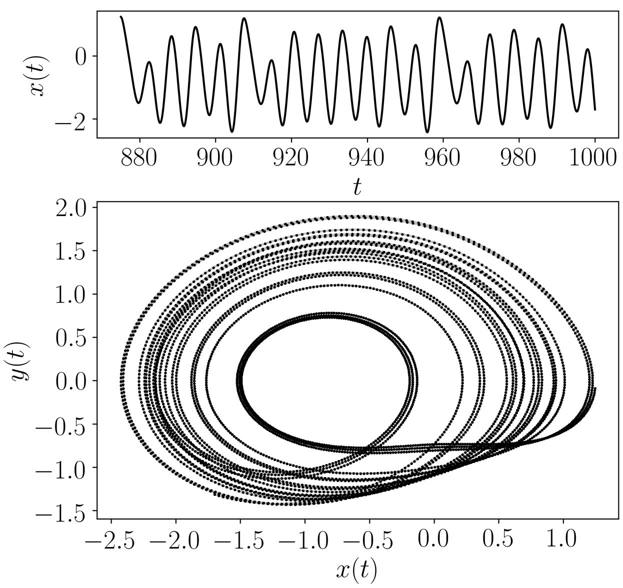

Figure 39

2.23 Double Scroll Attractor

The Double Scroll Attractor is defined [15] as

$$\begin{aligned}\frac{dx}{dt} &= y,\\ \frac{dy}{dt} &= z,\\ \frac{dz}{dt} &= -a(z + y + x - \operatorname{sgn}(x)),\end{aligned} \tag{41}$$

Dynamics	**Initial Cond.**	**Parameters**	**Sample Freq. (Hz)**	**Sample Domain**
Chaotic	$[x_0, y_0, z_0] = [0.01, 0.01, 0]$	$[a] = [0.8]$	20	[15000, 20000]
Periodic	$[x_0, y_0, z_0] = [0.01, 0.01, 0]$	$[a] = [1.0]$		

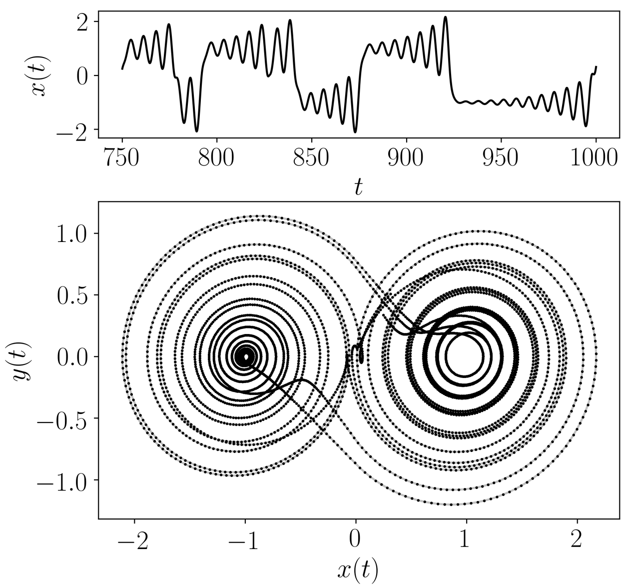

Figure 40

3 Delayed Flows

3.1 Mackey-Glass Delayed Differential Equation

The Mackey-Glass Delayed Differential Equation is defined as

$$x(t) = -\gamma x(t) + \beta \frac{x(t-\tau)}{1+x(t-\tau)^n} \tag{42}$$

with $\tau = 2$, $\beta = 2$, $\gamma = 1$, and $n = 9.65$. This was solved for 400 seconds with a sampling rate of 50 Hz. The solution was then downsampled to 5 Hz and the last 200 seconds were used as shown in Fig. 43.

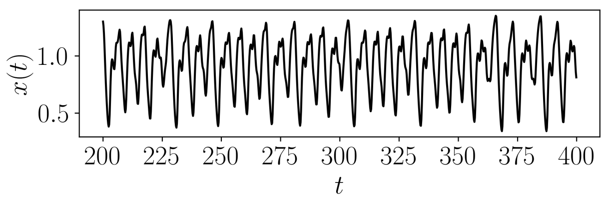

Figure 41

4 Periodic and Quasiperiodic Functions

4.1 Periodic Sinusoidal Function

The sinusoidal function is defined as

$$x(t) = \sin(2\pi t) \tag{43}$$

This was solved for 40 seconds with a sampling rate of 50 Hz.

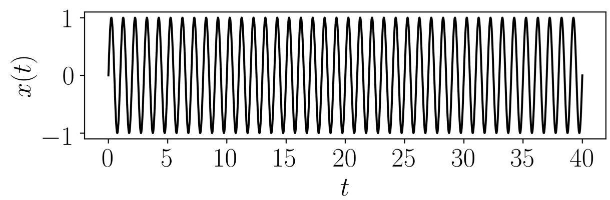

Figure 42

4.2 Quasiperiodic Function

This function is generated using two incommensurate periodic functions as

$$x(t) = \sin(\pi t) + \sin(t). \tag{44}$$

This was sampled such that $t \in [0, 100]$ at a rate of 50 Hz.

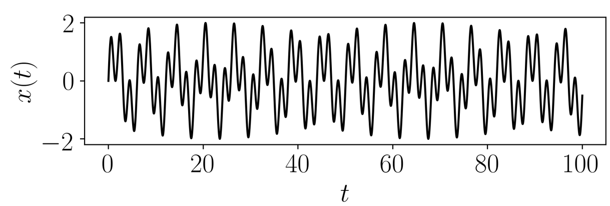

Figure 43

5 Driven Dissipative Flows

5.1 Driven Simple Pendulum

The point mass, driven simple pendulum with viscous damping is described as

$$\begin{aligned} \frac{d\theta}{dt} &= \omega, \\ \frac{d\omega}{dt} &= -\frac{g}{\ell}\sin(\theta) + \frac{A}{m\ell^2}\sin(\omega_m t) - c\omega, \end{aligned} \tag{45}$$

where $g = 9.81\ m/s^2$ is the gravitational constant, $\ell = 1\ m$ is the length of the pendulum arm, $m = 1\ kg$ is the mass of the point mass, $A = 5\ Nm$ is the amplitude of forcing, and ω_m is the driving frequency, where $\omega_m = 1\ rad/s$ for a periodic response and $\omega_m = 2\ rad/s$ for a chaotic response. The system was simulated for 300 seconds at a rate of 50 Hz and the last 100 seconds were used for the chaotic response as shown in the figure below.

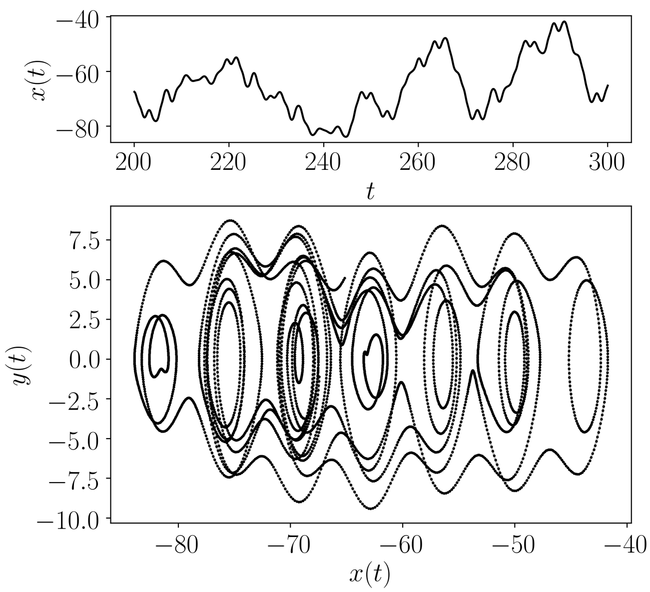

5.2 Base-excited Magnetic Pendulum

Let the total mass of the rotating components be M, the distance from the rotation center O to the mass center of the rotating assembly r_{cm}, and the mass moment of inertia of the rotating components about their mass center be I_{cm}. Further, assume that the magnetic interactions are well approximated by a dipole model with $m_1 = m_2 = m$ representing the magnitudes of the dipole moment. To develop the equation of motion,

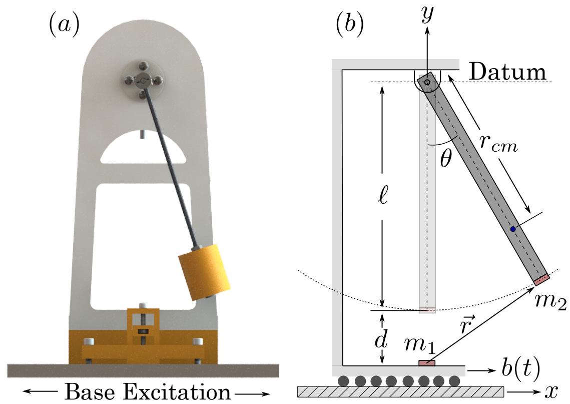

Figure 44: Rendering of experimental setup in comparison to reduced model, where $b(t) = A\sin(\omega t)$ is the base excitation with frequency ω and amplitude A, r_{cm} is the effective center of mass of the pendulum, d is the minimum distance between magnets $m_1 = m_2 = m$ (modeled as dipoles), and ℓ is the length of the pendulum.

we use Lagrange's equation (Eq. (56)), so the potential energy V, kinetic energy T, and non-conservative moments R are needed. In this analysis the damping moments and the moments generated from the magnetic interaction are treated as non-conservative. The potential and kinetic energy are defined as

$$\begin{aligned} T &= \frac{1}{2}M|\vec{v}_{cm}|^2 + \frac{1}{2}I_{cm}\dot{\theta}^2, \\ V &= -Mgr_{cm}\cos(\theta), \end{aligned} \tag{46}$$

where $\vec{v}_{cm}$ is the velocity of the mass center given by

$$\vec{v}_{cm} = r_{cm}\dot{\theta}\left[\cos(\theta)\hat{\epsilon}_x + \sin(\theta)\hat{\epsilon}_y\right] + A\cos(\omega t)\hat{\epsilon}_x. \tag{47}$$

In Eq. (49), $A\cos(\omega t)$ is introduced from the base excitation $b(t) = A\cos(\omega t)$ in the x direction with A as the amplitude and ω as the frequency and $\hat{\epsilon}_x$ and $\hat{\epsilon}_y$ are the unit vectors in the x and y directions, respectively.

The non-conservative moments are caused by the energy lost to damping. For our analysis, we consider only viscous damping τ_v with the resulting torque defined as defined as

$$\tau_v = \mu_v\dot{\theta} \tag{48}$$

where μ_v is the coefficient for viscous damping.

To begin the derivation of the torque induced from the magnetic interaction τ_m, consider two, in-plane magnets as shown in Fig. 46. From this representation, the magnetic force acting on each magnet is calculated as

$$F_r = \frac{3\mu_o m^2}{4\pi r^4}\left[2c(\phi-\alpha)c(\phi-\beta) - s(\phi-\alpha)s(\phi-\beta)\right],$$
$$F_\phi = \frac{3\mu_o m^2}{4\pi r^4}\left[s(2\phi-\alpha-\beta)\right], \tag{49}$$

where m_1 and m_2 are the magnetic moments, μ_o is the magnetic permeability of free space, and $c(*) = \sin(*)$ and $s(*) = \sin(*)$. Equation (51) assumes that the cylindrical magnets used in the experiment can be approximated as a dipole. These magnetic forces are then adapted to the physical pendulum with $\alpha = \pi/2$ and $\beta = \pi/2 - \theta$. Additionally, ϕ and r are calculated from θ, d, and ℓ as

$$\phi = \frac{\pi}{2} - \arcsin\left(\frac{\ell}{r}\sin(\theta)\right), \quad \text{and} \tag{50}$$

$$r = \sqrt{\left[\ell\sin(\theta)\right]^2 + \left[d + \ell(1-\cos(\theta))\right]^2}. \tag{51}$$

The moment induced by the magnetic interaction is then

$$\tau_m = \ell F_r \cos(\phi - \theta) - \ell F_\phi \sin(\phi - \theta). \tag{52}$$

Using τ_m from Eq. (54) and the non-conservative torque from Eq. (50), R is defined as

$$R = \tau_v + \tau_m. \tag{53}$$

Finally, the equation of motion for the base-excited magnetic single pendulum is found by substituting the above expressions into Lagrange's equation and noting that $L = T - V$

$$\frac{\partial}{\partial t}\left(\frac{\partial L}{\partial \dot{\theta}}\right) - \frac{\partial L}{\partial \theta} + R = 0. \tag{54}$$

The resulting equation of motion is put into state space form using Python's `sympy` package.

The following parameters are used:

$$[l, g, r_{cm}, I_o, A, \omega, c, q, d, \mu] = [0.1038, 0.208, 9.81, 0.18775, 0.00001919, 0.021 \text{ (0.022 for chaotic)}, 3\pi, 0.003, 1.2, 0.032, 1.257E-6], \tag{55}$$

where m (mass), l (length), g (gravity), r_{cm} (distance to center of mass), I_o (inertia about origin), ω (base excitation frequency), A (base excitation amplitude), c (viscous damping parameter) μ (universal magnetic constant), and d (minimum distance between magnets) are parameters with metric units (meters, seconds, radians, kilograms).

The system was simulated for 100 seconds at a rate of 200 Hz and the last 25 seconds were used for the chaotic response as shown in the figure below.

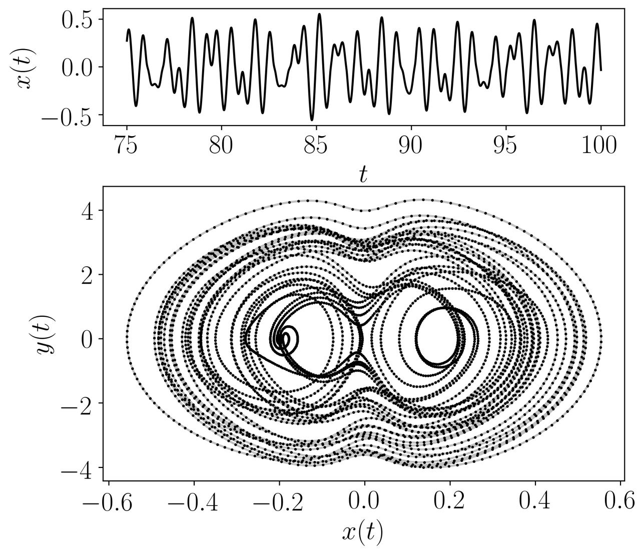
0.5
0.0
−0.5
x(t)
75
80
85
90
95
100
t
4
2
0
−2
−4
y(t)
−0.6
−0.4
−0.2
0.0
0.2
0.4
0.6
x(t)

5.3 Driven Van der Pol Oscillator

The Driven Van der Pol Oscillator is defined as

$$\begin{aligned} \frac{dx}{dt} &= y, \\ \frac{dy}{dt} &= -x + b(1 - x^2)y + A\sin(\omega t), \end{aligned} \tag{56}$$

Dynamics	**Initial Cond.**	**Parameters**	**Sample Freq. (Hz)**	**Sample Domain**
Chaotic	$[x_0, y_0] = [-1.9, 0.0]$	$[b, A, \omega] = [3.0, 5, 1.788]$	40	[7000, 12000]
Periodic	$[x_0, y_0] = [-1.9, 0.0]$	$[b, A, \omega] = [2.9, 5, 1.788]$		

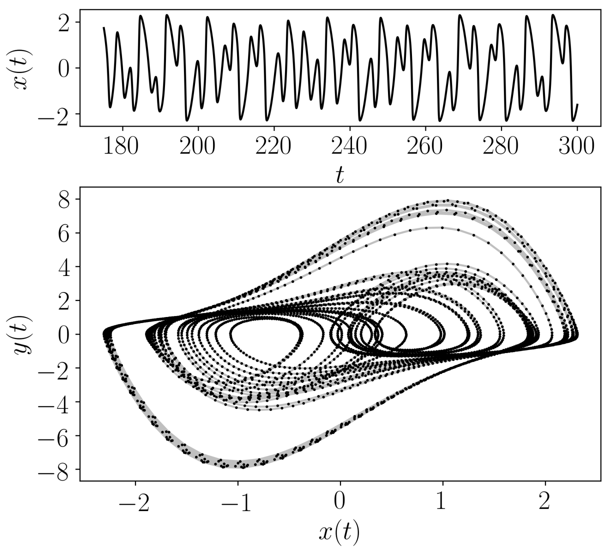

Figure 45

5.4 Shaw Van der Pol Oscillator

The Shaw Van der Pol Oscillator is defined as

$$\begin{aligned}\frac{dx}{dt} &= y + \sin(\omega t),\\ \frac{dy}{dt} &= -x + b(1 - x^2)y,\end{aligned} \tag{57}$$

Dynamics	Initial Cond.	Parameters	Sample Freq. (Hz)	Sample Domain
Chaotic	$[x_0, y_0] = [1.3, 0.0]$	$[b, A, \omega] = [1, 5, 1.8]$	25	[7500, 12500]
Periodic	$[x_0, y_0] = [1.3, 0.0]$	$[b, A, \omega] = [1, 5, 1.4]$		

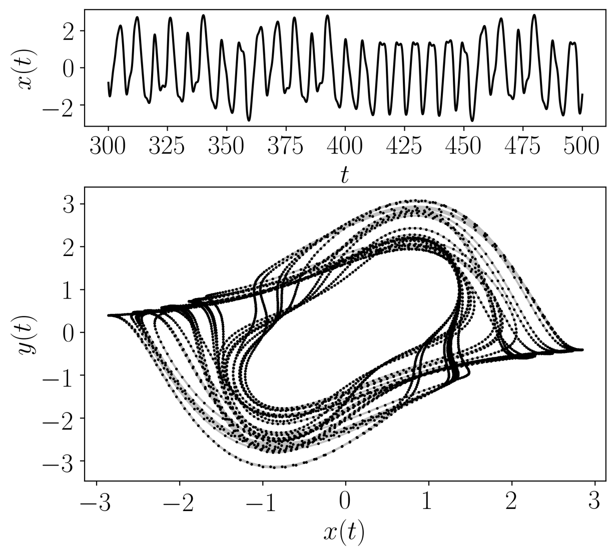

Figure 46

5.5 Duffing Van der Pol Oscillator

The Duffing Van der Pol Oscillator is defined as

$$\begin{aligned}\frac{dx}{dt} &= y,\\ \frac{dy}{dt} &= \mu(1-\gamma x^2)y - x^3 + A\sin(\omega t),\end{aligned} \tag{58}$$

Dynamics	**Initial Cond.**	**Parameters**	**Sample Freq. (Hz)**	**Sample Domain**
Chaotic	$[x_0, y_0] = [0.2, 0.0]$	$[\mu, \gamma, A, \omega] = [0.2, 8, 0.35, 1.2]$	20	[5000, 10000]
Periodic	$[x_0, y_0] = [0.2, 0.0]$	$[\mu, \gamma, A, \omega] = [0.2, 8, 0.35, 1.3]$		

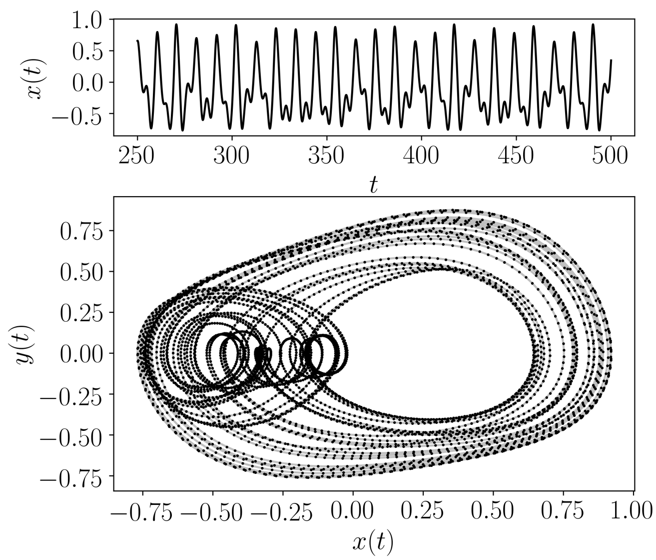

Figure 47

5.6 Forced Brusselator

The Forced Brusselator is defined as

$$\begin{aligned}\frac{dx}{dt} &= (x^2)y - (b+1)x + a + A\sin(\omega t),\\ \frac{dy}{dt} &= -(x^2)y + bx,\end{aligned} \tag{59}$$

Dynamics	Initial Cond.	Parameters	Sample Freq. (Hz)	Sample Domain
Chaotic	$[x_0, y_0] = [0.3, 2.0]$	$[a, b, A, \omega] = [0.4, 1.2, 0.05, 1.0]$	20	[5000, 10000]
Periodic	$[x_0, y_0] = [0.3, 2.0]$	$[a, b, A, \omega] = [0.4, 1.2, 0.05, 1.1]$		

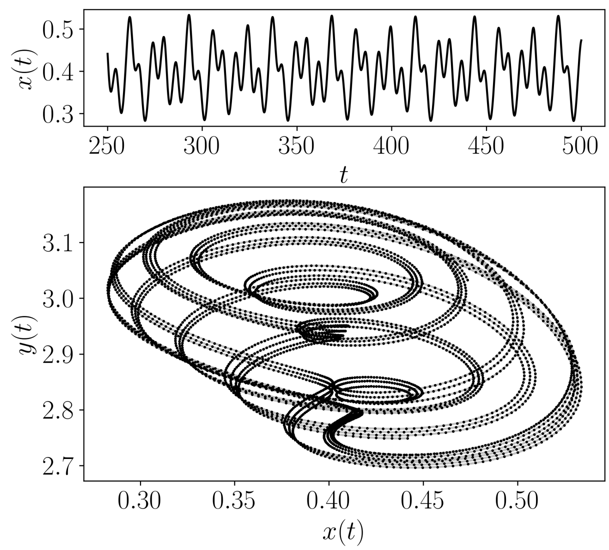

Figure 48

5.7 Ueda Oscillator

The Ueda Oscillator is defined as

$$\begin{aligned}\frac{dx}{dt} &= y,\\ \frac{dy}{dt} &= -x^3 - by + A\sin(\omega t),\end{aligned} \tag{60}$$

Dynamics	**Initial Cond.**	**Parameters**	**Sample Freq. (Hz)**	**Sample Domain**
Chaotic	$[x_0, y_0] = [2.5, 0.0]$	$[b, A, \omega] = [0.05, 7.5, 1.0]$	50	[20000, 25000]
Periodic	$[x_0, y_0] = [2.5, 0.0]$	$[b, A, \omega] = [0.05, 7.5, 1.2]$		

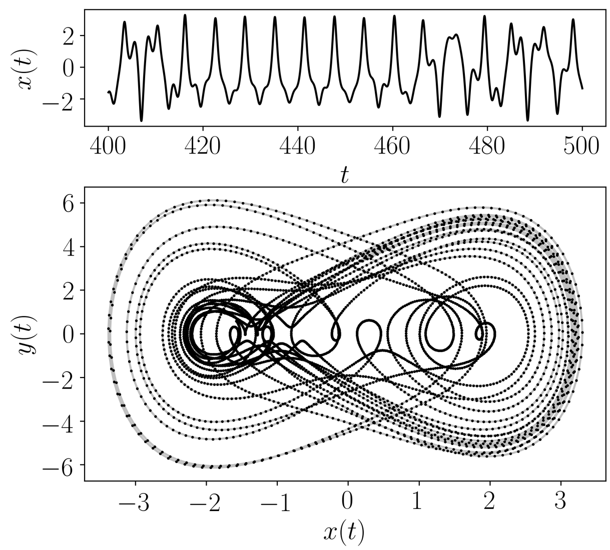

Figure 49

5.8 Duffings Two-Well Oscillator

The Duffings Two-Well Oscillator is defined as

$$\begin{aligned} \frac{dx}{dt} &= y, \\ \frac{dy}{dt} &= -x^3 + x - by + A\sin(\omega t), \end{aligned} \tag{61}$$

Dynamics	**Initial Cond.**	**Parameters**	**Sample Freq. (Hz)**	**Sample Domain**
Chaotic	$[x_0, y_0] = [2.5, 0.0]$	$[b, A, \omega] = [0.25, 0.4, 1.0]$	20	[5000, 10000]
Periodic	$[x_0, y_0] = [2.5, 0.0]$	$[b, A, \omega] = [0.25, 0.4, 1.1]$		

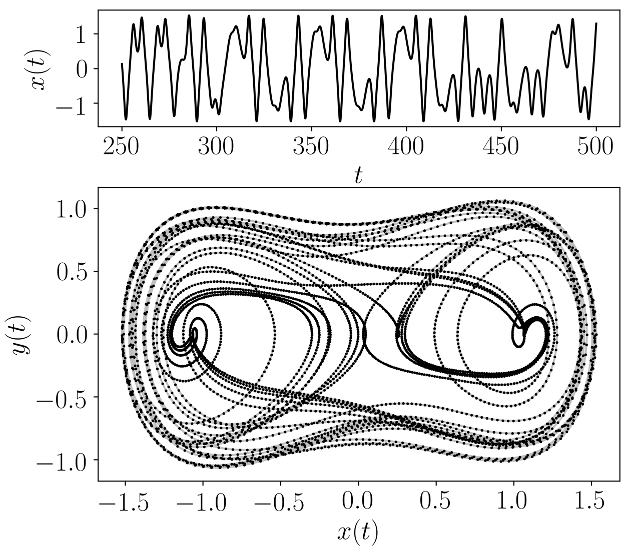

Figure 50

5.9 Rayleigh Duffing Oscillator

The Rayleigh Duffing Oscillator is defined as

$$\begin{aligned} \frac{dx}{dt} &= y, \\ \frac{dy}{dt} &= \mu(1-\gamma y^2)y - x^3 + A\sin(\omega t), \end{aligned} \tag{62}$$

Dynamics	**Initial Cond.**	**Parameters**	**Sample Freq. (Hz)**	**Sample Domain**
Chaotic	$[x_0, y_0] = [0.3, 0.0]$	$[\mu, \gamma, A, \omega] = [0.2, 4.0, 0.3, 1.2]$	20	[5000, 10000]
Periodic	$[x_0, y_0] = [0.3, 0.0]$	$[\mu, \gamma, A, \omega] = [0.2, 4.0, 0.3, 1.4]$		

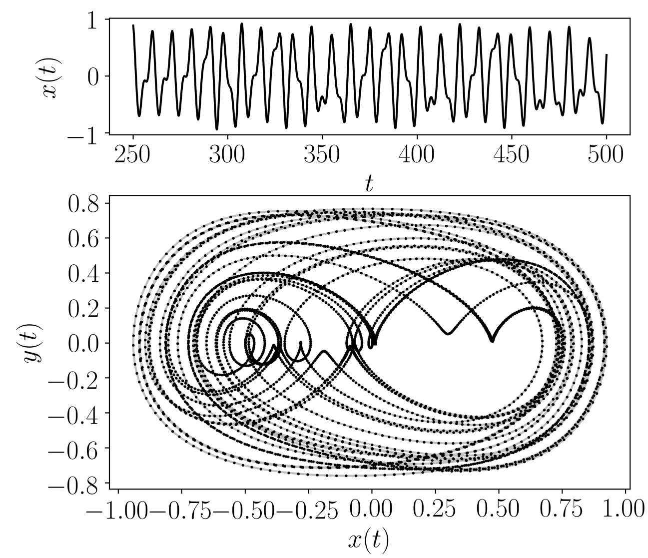

Figure 51

6 Human/Medical Data

6.1 EEG Data

The EEG signal was taken from andrzejak et al. [1]. Specifically, the first 5000 data points from the EEG data of a healthy patient from set A (file Z-093) was used and the first 5000 data points of a patient experiencing a seizure from set E (file S-056) was used (see figure below for case during seizure).

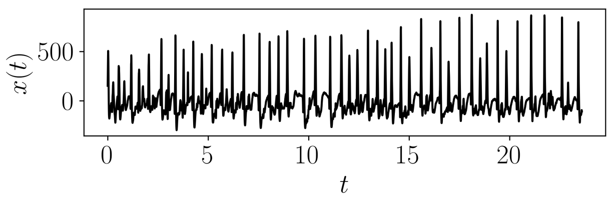

6.2 ECG Data

The Electrocardoagram (ECG) data was taken from SciPy's misc.electrocardiogram data set. This ECG data was originally provided by the MIT-BIH Arrhythmia Database [22]. We used data points 3000 to 5500 during normal sinus rhythm and 8500 to 11000 during arrhythmia (arrhythmia case shown below in figure).

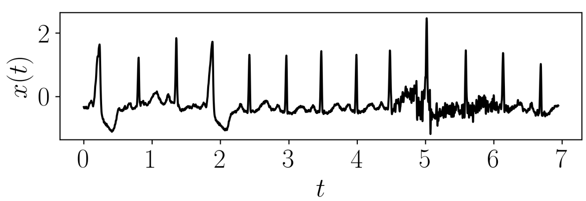

References

[1] Ralph G Andrzejak, Klaus Lehnertz, Florian Mormann, Christoph Rieke, Peter David, and Christian E Elger. Indications of nonlinear deterministic and finite-dimensional structures in time series of brain electrical activity: Dependence on recording region and brain state. *Physical Review E*, 64(6):061907, 2001.

[2] A. Arneodo, P. Coullet, and C. Tresser. Possible new strange attractors with spiral structure. *Communications in Mathematical Physics*, 79(4):573–579, dec 1981.

[3] V. I. Arnold. Small denominators. i. mapping the circle onto itself. *Izv. Akad. Nauk SSSR Ser. Mat.*, 1961.

[4] N. J. Balmforth and R. V. Craster. Synchronizing moore and spiegel. *Chaos: An Interdisciplinary Journal of Nonlinear Science*, 7(4):738–752, dec 1997.

[5] Schlögl Beck. Thermodynamics of chaotic systems. *Cambridge University Press*, 1995.

[6] J. M. Burgers. Mathematical examples illustrating relations occurring in the theory of turbulent fluid motion. *.Trans. Roy. Neth. Acad. Sci. Amsterdam.*, 1939.

[7] Ramanathan C., Abishek Arun R., K.V. Sriharsha, S. Hamsavaahini, Abirami R., J.N. Saranya, R. Subhathira, Kalaiselvan K., and N.R. Raajan. A new chaotic attractor from rucklidge system and its application in secured communication using OFDM. In *2017 11th International Conference on Intelligent Systems and Control (ISCO)*. IEEE, jan 2017.

[8] O. Chavoya-Aceves, F. Angulo-Brown, and E. Piña. Symbolic dynamics of the cubic map. *Physica D: Nonlinear Phenomena*, 14(3):374–386, mar 1985.

[9] Hsien-Keng Chen and Ching-I Lee. Anti-control of chaos in rigid body motion. *Chaos, Solitons & Fractals*, 21(4):957–965, aug 2004.

[10] MICHAEL CRAMPIN and BENEDICT HEAL. On the chaotic behaviour of the tent map. *Teaching Mathematics and its Applications*, 13(2):83–89, 1994.

[11] Marius-F. Danca. Hidden transient chaotic attractors of rabinovich–fabrikant system. *Nonlinear Dynamics*, 86(2):1263–1270, jul 2016.

[12] Robert Devaney. The gingerbreadman. *Algorithms*, 1992.

[13] Robert L. Devaney. A piecewise linear model for the zones of instability of an area-preserving map. *Physica D: Nonlinear Phenomena*, 10(3):387–393, mar 1984.

[14] Dickau. Lozi attractor. 1992.

[15] A.S Elwakil and M.P Kennedy. Chua's circuit decomposition: a systematic design approach for chaotic oscillators. *Journal of the Franklin Institute*, 337(2):251 – 265, 2000.

[16] Alexandre Goldsztejn, Wayne Hayes, and Pieter Collins. Tinkerbell is chaotic. *SIAM Journal on Applied Dynamical Systems*, 10(4):1480–1501, jan 2011.

[17] M. Hénon. A two-dimensional mapping with a strange attractor. *Communications in Mathematical Physics*, 50(1):69–77, feb 1976.

[18] Robert C. Hilborn. Chaos and nonlinear dynamics: an introduction for scientists and engineers. *Oxford, Univ. Press*, 2004.

[19] Yorke Kaplan. Functional differential equations and approximation of fixed points. *Springer*, 1979.

[20] J.-M. Malasoma. What is the simplest dissipative chaotic jerk equation which is parity invariant? *Physics Letters A*, 264(5):383–389, jan 2000.

[21] Robert M. May. Simple mathematical models with very complicated dynamics. *Nature*, 261(5560):459–467, jun 1976.

[22] George B Moody and Roger G Mark. The impact of the mit-bih arrhythmia database. *IEEE Engineering in Medicine and Biology Magazine*, 20(3):45–50, 2001.

[23] W. E. Ricker. Stock and recruitment. *Journal of the Fisheries Research Board of Canada*, 11(5):559–623, may 1954.

[24] Robert Shaw. Strange attractors, chaotic behavior, and information flow. *Zeitschrift für Naturforschung A*, 36(1):80–112, jan 1981.

[25] J.C. Sprott. Simplest dissipative chaotic flow. *Physics Letters A*, 228(4):271 − 274, 1997.

[26] R. Thomas. Deterministic chaos seen in terms of feedback circuits: Analysis, synthesis, "labyrinth chaos". *International Journal of Bifurcation and Chaos*, 9:1889–1905, 1999.

[27] S. Vaidyanathan, , Ch. K. Volos, K. Rajagopal, I. M. Kyprianidis, I. N. Stouboulos, , , and and. Adaptive backstepping controller design for the anti - synchronization of identical WINDMI chaotic systems with unknown parameters and its SPICE implementation. *Journal of Engineering Science and Technology Review*, 8(2):74–82, apr 2015.

[28] TAO YANG and LEON O. CHUA. PIECEWISE-LINEAR CHAOTIC SYSTEMS WITH a SINGLE EQUILIBRIUM POINT. *International Journal of Bifurcation and Chaos*, 10(09):2015–2060, sep 2000.